Identification of Multiple Power Quality Disturbances Problems in Wind-Grid Integration System

Muhammad Abubakar*‡, Yue Shen*, Hui Liu* and Fida Hussain*

* School of Electrical and Information Engineering, Jiangsu University, Zhenjiang 212013, China

(mabubakarqazi@gmail.com, shen@ujs.edu.cn, amity@ujs.edu.cn, fida.hussain07@yahoo.com)

‡ Corresponding Author; Muhammad Abubakar, School of Electrical and Information Engineering, Jiangsu University, Zhenjiang 212013, China, Tel: +86 -18652841652, mabubakarqazi@gmail.com

Received: 19.07.2019 Accepted:07.09.2019

Abstract- In the modern era, the more usage of the non-linear load has increased the importance of power quality (PQ) monitoring. This paper purposes the novel algorithm based on Multivariate singular spectral analysis (MSSA), Wavelet Packet Decomposition (WPD) and 1-Dimensional Convolution Neural Network (1-D-CNN) for monitoring, mitigation, and classification of power quality disturbances (PQDs). Twelve types of synthetic and simulated single and multiple PQDs data are generated from MATLAB R2017b and Modified IEEE 13-bus system using wind energy penetration. In this research, MSSA and WPD are decomposed into four levels to extract the statistical features such as energy, entropy, standard deviation, root mean square, skewness, and kurtosis. The experimental results are well explained to compare the best-suited feature extraction technique in terms of feature extraction accuracy and computational complexity. Optimally selected features are fed to a convolution neural network (CNN) based softmax classifier for classification of PQ disturbances. The proposed algorithm is also tested under no noise and 20 dB to 50 dB noisy environment. The performance of the proposed method is compared with recently published articles to justify the competency of this study. The results show that the proposed framework has obtained reliable highest classification accuracy.

Keywords Power quality disturbances, Wavelet packet decomposition, multivariate singular spectral analysis, convolution neural network, wind distributive system.

1. Introduction

The introduction of renewable energy technologies in recent time widely opens the researches in many fields. Power quality (PQ) problems are one of the major concerns that arise from the involvement of renewable sources and its interconnection with power grids [1-3]. Among different sources of renewable distribution generation (DG), the usage of wind generation is increasing. Due to the large penetration in DG based on wind energy. The synchronization problems between the power grid and wind destructive system may increase. As a result, many PQ disturbances (PQDs) such as notch, sag, harmonics, swell and their multiples may malfunction the protection system and shut-down the entire system [4, 5].

In order to mitigate these issues, PQ disturbances identification and monitoring is very important so that synchronization between conventional grid and renewable energy sources can be made smooth and stable [6]. In general, the identification and monitoring of PQ disturbances consist of three parts, feature extraction, feature selection and classification [7, 8]. Many signal processing techniques have been assessed such as, Fourier transform (FT), Fast Fourier transform (FFT), Short-time Fourier transform (STFT) and Discrete Fourier transform (DFT) for the detection and feature extraction [9-11].

Wavelet and multiresolution analysis (MRA) is one of the traditional signal processing techniques, which provides variable size window such as a long window for low-frequency components and short window for high-frequency components. As a result, it provides excellent time-frequency resolution [12]. WT helps to analyze the PQ event and classifying the low and high-frequency issues of

PQ disturbances. However, the calculation of appropriate sampling frequency and mother wavelet is one of the key issues that arise in WT to find out the suitable frequency components [13]. Wavelet packet decomposition (WPD) decomposes the scale and wavelet coefficients at a specific level. Which provides detail and accurate information about time-frequency resolution. WPD is better decomposition technique than DWT due to the fix frequency band [14].

Singular spectral analysis (SSA) based on M lagged copies of time series. The estimation of the correlation matrix relies on Karhunen-Loève decomposition. The eigenvectors of this matrix are called empirical orthogonal functions (EOFs) [15]. SSA decomposes the time-series signal into various fluctuation trends, a small number of signals, oscillation, and noises. Instead of reducing the dimension of data, SSA smooths the spectral profile of given data which improves the feature extraction, and classification accuracy can be enhanced accordingly [16, 17]. Additionally, Multiscale SSA (MSSA) is the extension of SSA and applied to many applications such as hyperspectral imaging(HIS), bearing fault diagnosis physiological signals, geophysics, murmur detection of a heart sound, vibration signal, and economic data [18-23].

In, doubly fed induction generator (DFIG) based wind grid system is utilized for the generation of PQ disturbance and mathematical morphology (MM) is applied for the detection of PQ issues. This technique eliminates the noise with high computational speed but the performance is critically depending on the parameters of MM [24]. In, probabilistic PQ indices are proposed for the DG system [25]. In [26], hyperbolic S-transform (ST) and decision tree based classifier are utilized and PQ disturbances are generated due to the load variation and environment situations in DG. In [27], ST for feature extraction and least square support vector machine (LS-SVM) for classification is proposed for PQ disturbances generated from 17-bus test system. Diverse extreme learning machine (DELM) is used for the trasient stability classification problem [28]. İn [29], Deep convolution neural network (DCNN) based classifier is utilized for the efficient classification of solar array detection in aerial imagery. Multi resolution analysis (MRA) used for extracting FFT coefficient for diagonsis task [30].

In this study, twelve types of single and multiple PQ disturbances are generated using the modified IEEE 13 bus system with a wind grid integration system [31]. The three-phase disturbances are segmented into single-phase and the feature set is computed through the MSSA and WPD techniques. Deep Convolution neural network (DCNN) based softmax classifier is used for efficient classification. A range of Gaussian noises is added in the signals (20 dB-50db) and support vector machine (SVM) classifier is also utilized to check the robustness of the proposed algorithm.

This article is organized as follows: Section 2 explains the proposed feature extraction methods, classifier, feature selection based on statistical parameters and proposed classifier. Section 3 describes the experiment. Section 4 explicates the results and discussion and finally, section 5 concludes the research work.

2. Methodology

2.1. Discrete Wavelet Transform

Generally, PQ disturbances are non-stationary due to the sudden change in voltage, current, and magnitude of the signal [32]. Discrete Wavelet Transform (DWT) can extract both time and frequency information, as well as reduce the computational complexity [33]. DWT decomposes the discrete-time signal $x[n]$ into different levels of wavelet coefficients. The important factor is to choose a suitable mother wavelet. Firstly, the appropriate number of decomposition levels are picked, g_m. Then, this initial level discrete-time signal passes through the High Pass (HP) and Low Pass (LP) filters. Figure 1 demonstrates the detailed mechanism of DWT. The high-frequency component (detail coefficients) are provided by the HP filters of their respective level (D1) and LP filter provides the low-frequency component (approximation coefficients *A1*) of the discrete-time signal, followed by the process of down-sampling by 2. the scale $\varphi(t)$ and wavelet $\omega(t)$ of approximate l and detail coefficients h for a signal $x[n]$ can be represented as:

$$\varphi(t) = \sqrt{2}\sum_{n} h(n)\varphi(2t-n) \tag{1}$$

$$\omega(t) = \sqrt{2}\sum_{n} l(n)\omega(2t-n) \tag{2}$$

In the next level, the A_g is set as $x[n]$ and g_m is increased by 1. The above mentioned process repeats until g reaches the limit of the selected number of levels, as shown in Fig.1.

2.2. Wavelet Packet Decomposition

WPD is the extension DWT, such as the detail coefficients D_g also decompose as well as with the decomposition of A_g. The slight difference increases the number of wavelet coefficients by 2^g rather than $g+1$ in DWT. This change effects to achieve better frequency

resolution for the decomposition of the signal [34]. DWT may miss important information at high-frequency components. This detail is shown in Fig.2.

2.3. Multiclass Singular spectral analysis

The multiclass singular spectral analysis is another method for feature decomposition of nonstationary signals of PQ disturbances [15]. MSSA method consists of generally four steps. 1) Embedding 2) singular value decomposition (SVD) 3). Grouping 4). Reconstruction of the signal.

Assume that we have uniformly sampled PQ disturbance, which is a 1-D signal in a vector array A define as $A=\left[a_1,a_{2,\ldots},a_N\right]^T\in\mathcal{R}^N$ of length N where N is $b-\frac{1}{2}W\le i\le b+\frac{1}{2}W$. where b is the position and window size W $\left(1<W<N\right)$. The trajectory matrix C of the matrix A can be formulated as

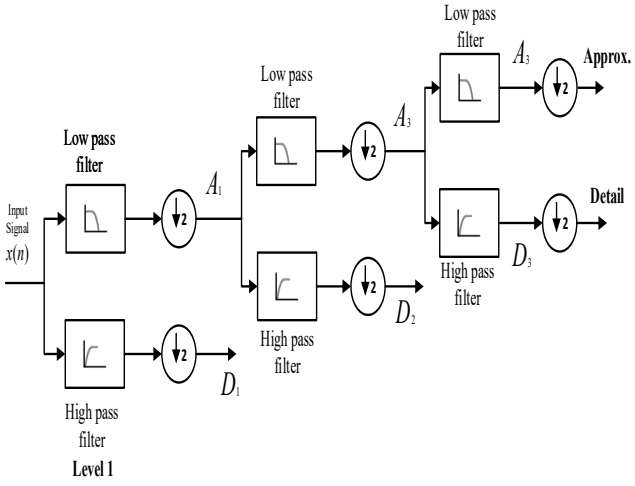

Figure 1. Decomposition of DWT for level

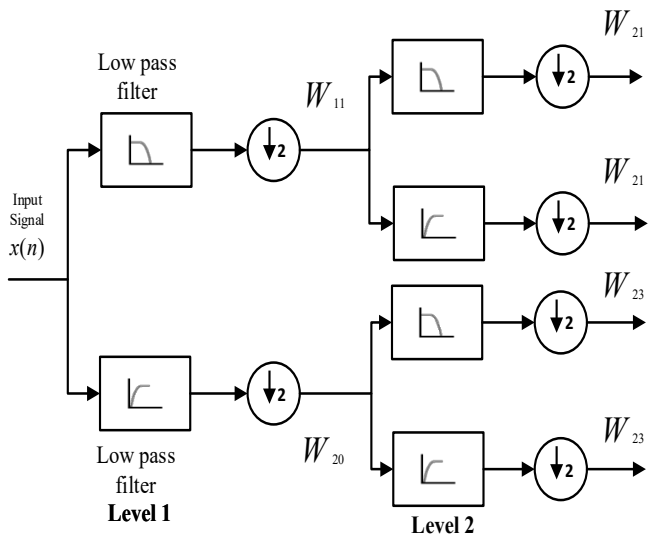

Figure 2. Decomposition of WPD for level 2

$$C=\begin{pmatrix} a_1 & a_2 & \cdots & a_K \\ a_2 & a_3 & & a_{K+1} \\ \vdots & \vdots & \ddots & \vdots \\ a_L & a_{L+1} & \cdots & a_N \end{pmatrix} \tag{3}$$

$$C=\left(c_1,c_2,\ldots,c_K\right) \tag{4}$$

Each column of C mapped to lagged vector K, that is $c_K=\left[a_k,a_{k+1},\ldots,a_{k-L+1}\right]^T\in\mathcal{R}^L$, where $k\in\left[1,K\right]$ and $K=N-W+1$. The covariance matrix keeps the whole information about input signals.

The lagged covariance matrix S is obtained from the trajectory matrix C, $S=CC^T$, its eigenvalues are calculated and sort in descending order as, $\left(\lambda_1\ge\lambda_2\ge\ldots\lambda_L\ge0\right)$, and equivalent eigenvectors be $\left(U_1,U_2,\ldots,U_L\right)$, and the trajectory matrix after SVD is presented as

$$C=C_1+C_2+,\ldots,C_d$$

Where $d\le W$ is the rank of matrix C but for simplicity, we consider $d=W$. As it can be noted, trajectory matrix C is a combination of several matrices. Each matrix $X_l\,|\,l\in\left[1,W\right]$ is called an elementary matrix and it is equivalent to its respective eigenvalue, the decomposition of the signal is defined by

$$X_l=\sqrt{\lambda_l}u_l^b\left(v_l^b\right)^T \tag{5}$$

Where v_l^b is define as

$$v_l^b=\frac{X^Tu_l^b}{\sqrt{\lambda_l}} \tag{6}$$

U and V matrices are denoted as the matrix of empirical orthogonal functions and the matrix of principal components respectively at a selected position of b.

$$U=\left(u_1^b,u_2^b,\ldots,u_L^b\right)\in\mathcal{R}^{L\times L} \tag{7}$$

$$V=\left(v_1^b,v_2^b,\ldots,v_L^b\right)\in\mathcal{R}^{L\times L} \tag{8}$$

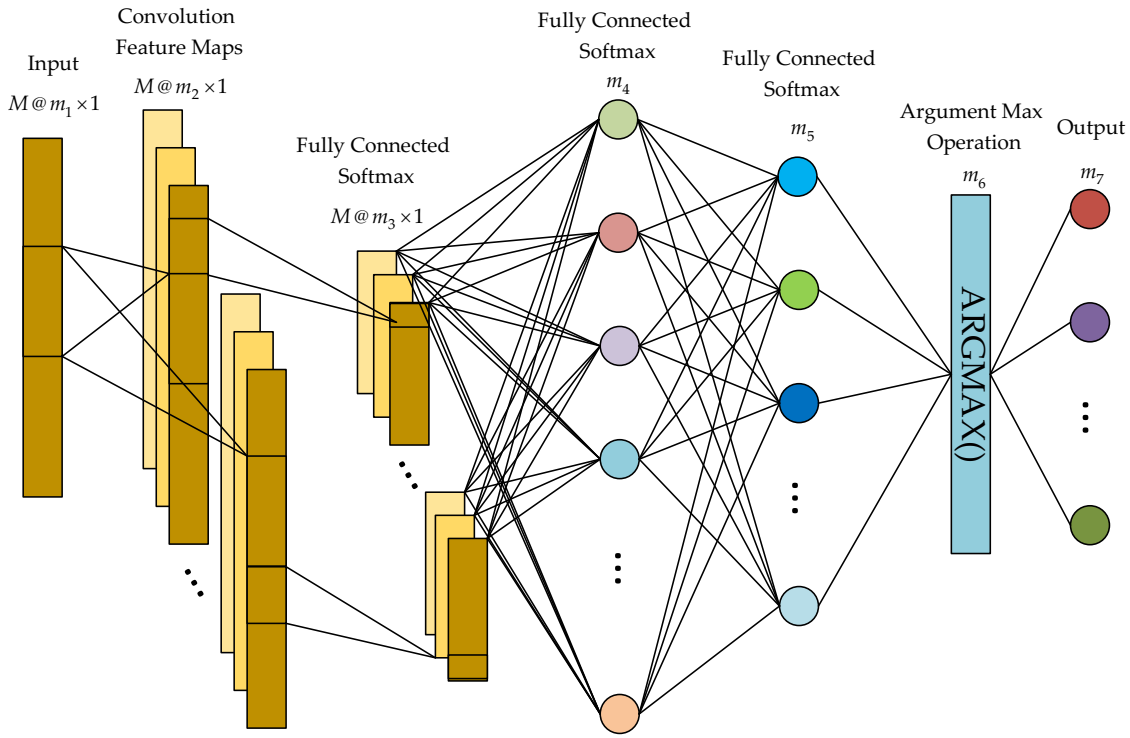

Figure 3. The comprehensive architecture of 1-D Convolutional neural network

2.4. Convolution neural network

In a wide context, Convolution neural network (CNN) is feature extraction and classification neural network topology. CNN can become complex with feature extraction and classification capabilities. The complex architecture of CNN can consist of multiple layers that extract different features from the PQDs [35]. Fewer examples of CNN complex architecture for different applications can be seen from the literature [36, 37]. In general, CNN is implemented in 2-dimensional with multi-dimensional kernels and complex configuration. Our network is further refined by adding dropout and regularization [38]. The PQDs data can be classified in a single dimension. In this paper, only the classification layer (softmax layer) with max pooled layer is utilized, which make the network simple for the classification of PQDs.

However, the architecture of 1-DCNN comprises of input, the convolution layer connected with network max pooling that feeds to fully connected softmax and output layers that are shown in Fig.3. the initial kernel was set at 24 for MSSA and 64 for WPD decompositions. The training process of CNN consists of forward propagation and backpropagation. Forward propagation trains the data for the classification and backpropagation is utilized to upgrade the training parameters to improve the classification accuracy.

2.4.1. Forward propagation

For (L+1) layer CNN network, m_1 is the input layer and m_7 is the output layer, l is the current layer, m_2 to m_6 numerous hidden units of convolution layer, max pooling layer, fully connected layers, and regularization layer, and expressed as:

$$w_n^l = \sum_{i=1}^{M} w_i^{l-1} * j_{in}^l + b_n^l \tag{9}$$

Where w_i^{l-1} is the convolution feature map of the previous layer. w_i^{l-1} is convolution feature map of current layer, *M is the number of input features.* b_n^l is the additive bias vector. '*' is the convolution operator. The output can be written as

$$z_n^l = f_n\left(w_n^l\right) \tag{10}$$

z_n^l is the output, f_n is the non-linear function, rectified linear units (ReLU) is a widely used non-linear operator and used as an activation function in this study. The advantage of this function is, it accepts the output of neuron if positive means it does not active all the neurons at the same time and converts all negative inputs to zero, which makes it efficient gradient propagation and low computational burden. *max(w)* function is used in pooling layer, fully connected layer with softmax layer is connected to the output layer as CNN is a multiclass classifier, the softmax layer is expressed as:

$$\delta(z)_n = \frac{e^{z_n}}{\sum_j^J e^{z_j}}, n = 1,...,J \quad (11)$$

Where z_n is the input from a fully connected layer, J is the number of classes or softmax layer units.

2.4.2. Backpropagation:

Backpropagation is used to tune the trainable parameters and the gradient descent method is used for this purpose. The output of max pooling layer is connected to backpropagation to sense the errors. The mean square error of the output can be calculated as:

$$E_q = \sum_{l=1}^{N_c} \left(z_l^l - t_l^q \right)^2$$

l is the number of classes and q is the input vector and t_l^q is the corresponding target and $\left[z_1^l, \ldots, z_q^l \right]$ is the output vector.

2.5. Feature extraction

The efficient feature extraction from the preprocess PQDs is very important to improve the classification accuracy [39]. In this paper, features are extracted and selected through the MSSA, WPD and statistical parameters. The use of all input data coefficient may decrease the classification accuracy and increase the computation load. Therefore, the statistical parameters such as energy, entropy, standard deviation, mean, kurtosis, and skewness are chosen [9]. For each decomposition technique, the total number of features obtained per phase is 24 for MSSSA and 64 for WPD decomposition technique. The mathematical relationship of these statistical parameters are given as

1) The coefficients of Energy for all sub-bands

$$E_{ki} = \sum_{j=1}^{N} \left(\left| X_{ij} \right|^2 \right) \quad (12)$$

2) The coefficients of Entropy for all sub-band,

$$ET_{ki} = -\sum_{j=1}^{N} X_{ij}^{\ 2} log\left(X_{ij}^{\ 2} \right) \quad (13)$$

3) The coefficients of Standard deviation for all sub-bands,

$$\sigma_{ki} = \left(\frac{1}{N} \sum_{j=1}^{N} \left(X_{ij} - \mu_i \right)^2 \right)^{\frac{1}{2}} \quad (14)$$

4) The coefficients Mean (signal) value for all sub-band,

$$\sigma_{ki} = \left(\frac{1}{N} \sum_{j=1}^{N} \left(X_{ij} - \mu_i \right)^2 \right)^{\frac{1}{2}} \quad (15)$$

5) The coefficients of Kurtosis for all sub-band,

$$KT_{ki} = \sqrt{\frac{N}{24}} \left(\frac{1}{N} \sum_{j=1}^{N} \left(\frac{X_{ij} - \mu_i}{\sigma_i} \right)^4 - 3 \right) \quad (16)$$

6) The coefficients of Skewness for all sub-band,

$$SN_{ki} = \sqrt{\frac{1}{6N}} \sum_{j=1}^{N} \left(\frac{X_{ij} - \mu_i}{\sigma_i} \right)^3 \quad (17)$$

2.6. Proposed Methodology

The proposed methods are divided into three sections 1) feature extraction 2) feature selection 3) classification. Firstly, the two selected feature extraction techniques are compared in terms of feature extraction accuracy and computational speed. Four level decomposition is used for these two methods. Secondly, optimal features are chosen through statistical parameters. And lastly, the optimally selected features are fed to the CNN based softmax classifier for the classification of PQDs. The detail of the proposed methods is shown in Fig. 4.

3. Experiments

3.1 Generation of PQ disturbances dataset by modified IEEE 13 node system

To generate the typical PQ disturbances, a modified IEEE 13 node bus with wind distribution system is selected [31]. The parameters of the original system are 50 Hz, 5 MVA of two voltage levels i.e. 4.16 kV and 0.48 kV with balanced and unbalanced loads with no renewable energy (RE) sources. This modified model with wind energy penetration is simulated in MATLAB/Simulink to produce the dataset 1 and some of the simulated PQ disturbances are shown in Fig. 6. In dataset 1, 5390 samples were created with a sampling frequency of 10 kHz for 12 types of PQ disturbances. Two wind turbines of 1.5 MV each are added at bus 680 that are shown in Fig. 5 and they are connected through the transformer T-2 and an 8 km overhead transmission line. The transmission line has the following parameters. R_0 (zero sequences) resistance 0.413 Ohms/km,

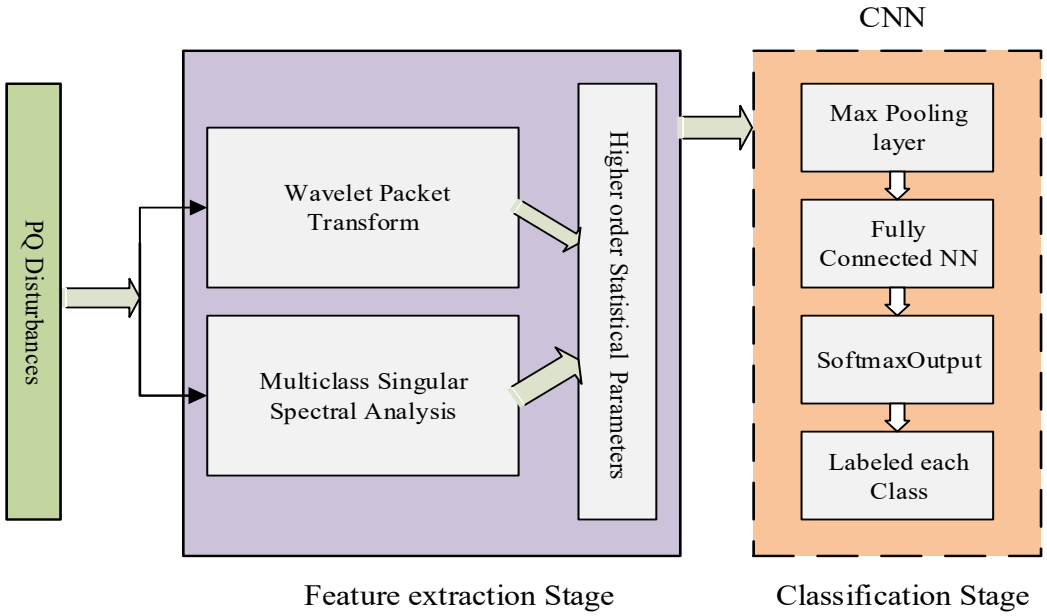

Figure 4. Block diagram of the proposed scheme

and R_1 (positive sequence) resistance 0.1153 Ohms/km, C_0 capacitance 5.09×10^{-9} F/km and C_1 capacitance 11.33×10^{-9} F/km and L_0 inductance 3.3×10^{-3} H/km and L_1 inductance 1.05×10^{-3} H/km, respectively. The location of modification in the IEEE 13 bus system is presented in Table 1.

Three-phase voltage sag and swell are generated by multistage and line to line faults, and line to line faults between two phases at generation end. The three-phase voltage notch, oscillatory transients, harmonics, flickers, and impulsive transients are generated by the three-phase nonlinear load, three-phase capacitor bank, arc furnace, and lightning at distributive end respectively. Multiple PQ disturbances are generated from their combinations.

Table 1. System load and data status of the modified IEEE bus system.

Bus Nodes	Load Model	Load		Capacitor Bank	Modified data
-	-	kW	kVAr	kVAr	-
634	Y-PQ	400	290		-
645	Y-PQ	170	125	-	-
646	D-Z	230	132	-	-
652	Y-Z	128	86	-	-
671	D-PQ	1155	660	-	-
675	Y-PQ	843	462	600	Switching Fault
692	D-I	170	151	-	-
611	Y-I	170	80	100	Switching Fault
632-671	Y-PQ	200	116		
650 680					- Grid WG/non-linear load

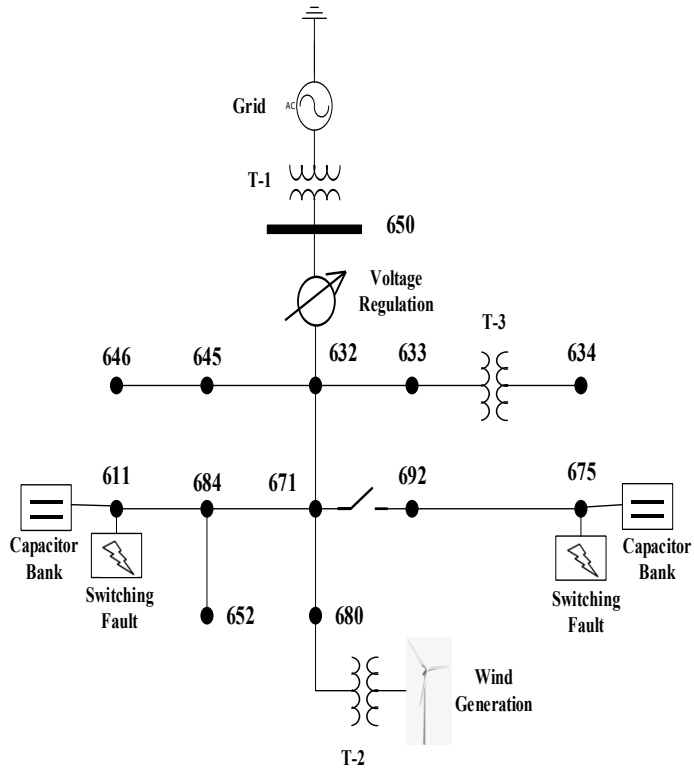

Figure 5. Modified IEEE 13 bus system with Wind system connected at node

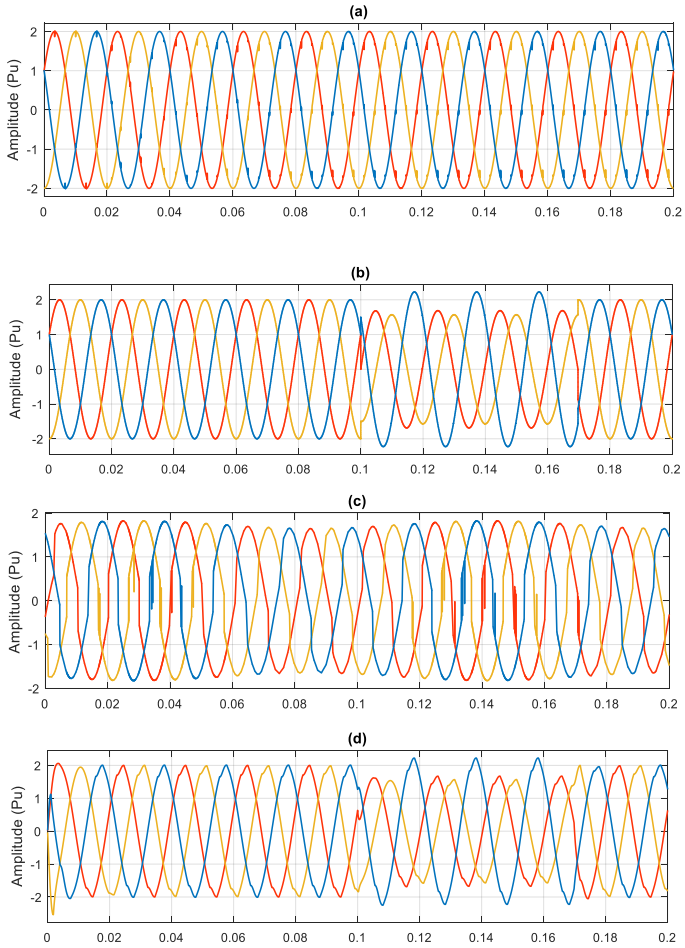

Figure 6. Three-phase PQDs generation from Wind grid integration model (a) voltage notch (b) voltage sag and swell (c) voltage flicker (d) harmonics with sag and swell

3.2 Generation of synthetic PQ disturbances dataset

The synthetic PQ disturbances dataset were generated based on parametric equations model [8]. This model was simulated in MATLAB 2017b and PSCAD/EMTDC software. Each waveform was created with specific parameters, the sampling points are 2000, 10 cycles, 10 kHz sampling frequency. The 12 types of synthetic PQ disturbances are shown in Fig.7.

In this study, Gaussian noise was also added (20 dB to 50 dB) to analyze the classification accuracy. Some of the noisy (50dB) PQ disturbances are presented in Fig. 8. This algorithm was tested more than 20 times to confirm the classification performance. Training and testing sets were separated by 75% and 25% respectively.

However, the number of decomposition levels for WPD is also four that resulted in $2^g = 2^4 = 16$ sub-bands. In Table 2, details of frequencies in sub-bands of WPD are discussed with corresponding relations to MSSA sub-bands. WPD has eleven additional sub-bands than the other decomposition methods which would result in features difference. Figure 9 and 10 show the details about PQ disturbance signals decomposition using MSSA, and WPD.

Table 2. Detail of sub-bands frequencies of 4 level WPD and MSSA.

Sub-band No.	Decomposition Signal	Frequency Range (Hz)	MSSA level
i	SB40	0-3.1	APP.4
ii	SB41	3.1-6.3	DC.4
iii	SB42	6.3-9.4	DC.3
iv	SB43	9.4-12.5	-
v	SB44	12.5-15.6	DC.2
vi	SB45	15.6-18.8	-
vii	SB46	18.8-21.9	-
viii	SB47	21.9-25.0	-
ix	SB48	25.0-28.1	DC.1
x	SB49	28.1-31.3	-
xi	SB4A	31.3-34.3	-
xii	SB4B	34.3-37.5	-
xiii	SB4C	37.5-40.6	-
xiv	SB4D	40.6-43.8	-
xv	SB4E	43.8-46.9	-
xvi	SB4F	46.9-50.0	-

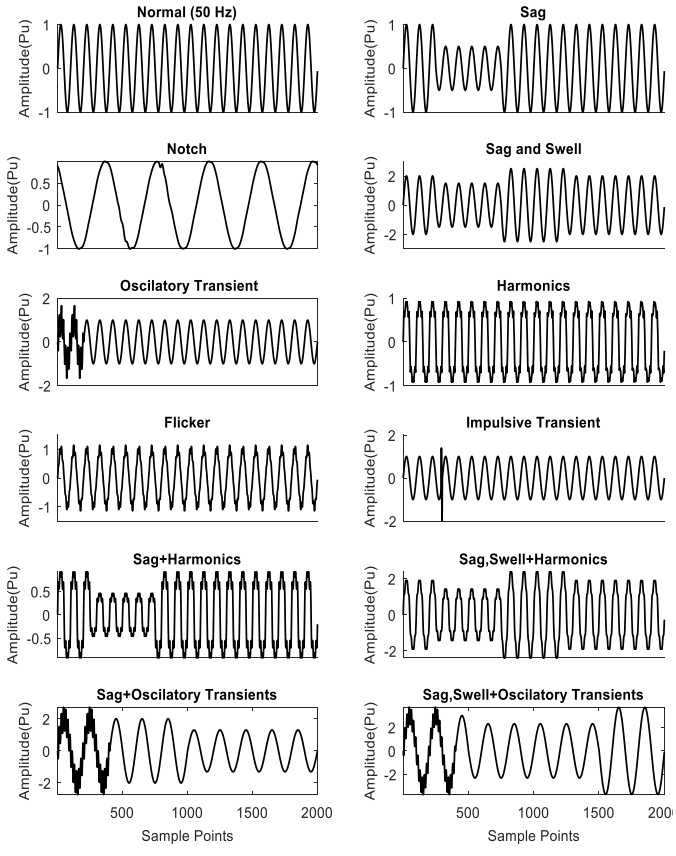

Figure 7. Twelve types of synthetic PQ disturbance

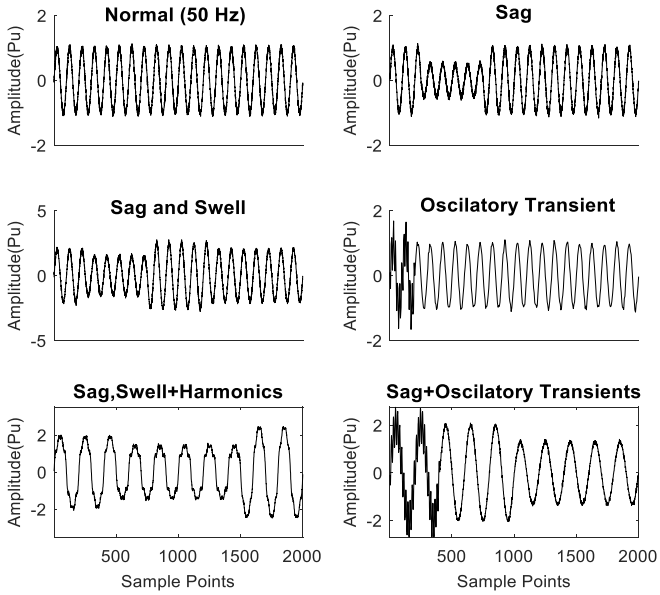

Figure 8. The waveform of PQ disturbance (50dB)

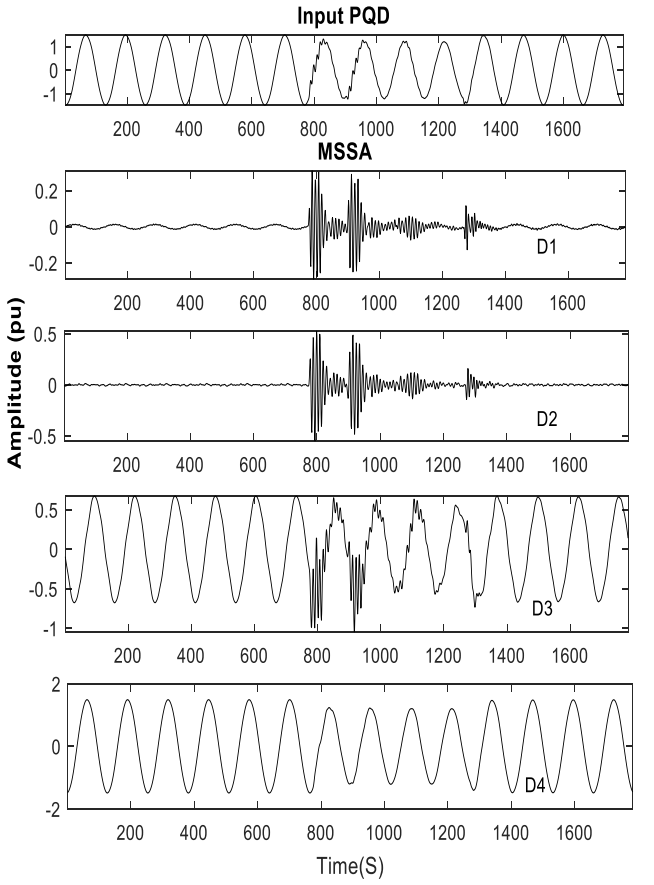

Figure 9. PQ disturbance four level decomposition using MSSA

4. Results and Discussion

In this section, the results of two selected feature extraction techniques with CNN based softmax classifier are discussed. Two different datasets with different noise levels are used to evaluate the outcomes of the classifier. The first dataset is based on the syndetic PQ disturbances and the second dataset is generated from modified IEEE 13 bus system with the wind-grid distributive system.

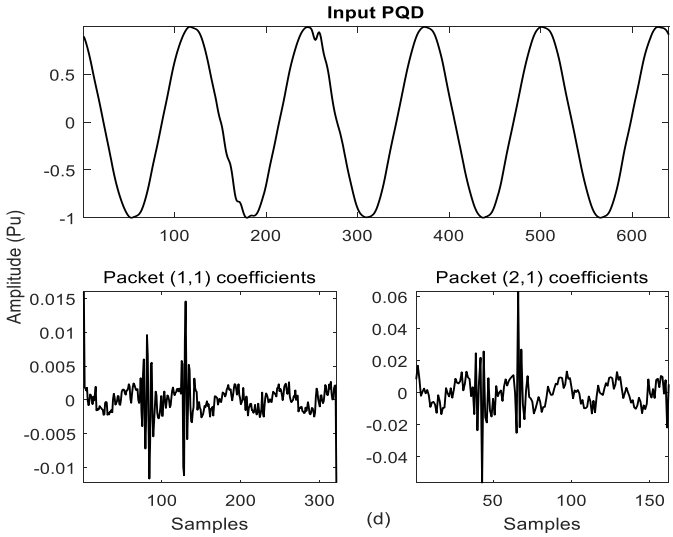

Figure 10. PQ disturbance decomposition using WPD

In Table 3, the classification accuracies of CNN based softmax classifier along with MSSA and WPD decomposition technique are presented. The classification accuracies with dataset 1 (synthetic PQDs), dataset 2 (Modified IEEE 13 bus system with wind grid distributive system-generated PQDs) and different noise levels are also described. WPD has higher classification accuracy (99.8%) as compared to MSSA (99%) for noiseless condition and dataset 1. This algorithm also shows significance classification performance under noisy environment and dataset 2. Table 2 well explained better classification results. It can be observed that the maximum frequency sub-bands are of MSSA i.e. detail DC1, 25 to 28.1 Hz. However, WPD will produce much more features in the frequency range of 25-50 Hz, which will result in the depth insight between the classes. It means that WPD results in fining the decomposition for the highest frequencies using lower scale levels as compared to MSSA.

For the same number of decomposition levels, WPD generates a fine range of features. While other decomposition methods require a high number of decomposition levels to achieve the same distinctive number of features. In case the of MSSA, The two parameters decide an effective feature extraction of PQDs. Firstly, the value α determines the total number of eigenvalues extracted during the decomposition stage. Secondly, the eigenvalue group (EVG) describes how extracted components are grouped to extract the best features. If it contains all the eigenvalues, then it extracts all features in the PQD signal. If the EVG dismisses the small value of eigenvalues, then extracted features are more

Table 3. Classification accuracy (%) of PQ disturbances

Power Quality Disturbances	Class Labelled	Training/ Testing sets	MSSA				WPD			
			Dataset 1		Dataset 2		Dataset 1		Dataset 2	
			0 dB	50 dB	0 dB	50 dB	0 dB	50 dB	0 dB	50 dB
Normal	C_1	200	100	99	100	99	100	100	100	100
Sag	C_2	200	100	99	100	99	100	99	100	99
Notch	C_3	200	99	98	99	98.5	100	99	100	99
Flickers	C_4	200	98	97	97.8	97.1	100	99	100	98.8
Impulsive Transients	C_5	200	99	99	98.9	97.9	100	99	99.8	99
Oscillatory Transients	C_6	200	99	98	99	98.5	99	99	99.7	98.7
Harmonics	C_7	200	99	99	98.4	97.3	99.5	99.1	99.6	99
Sag with Swell	C_8	200	99	98	98.1	97.1	100	99.5	99.8	99
Sag with Harmonics	C_9	200	98	98	98	96.9	99.7	98.2	99.6	97.9
Harmonics with Sag and Swell	C_{10}	200	99	98	98.9	97.4	99.6	99.2	99.5	99
Sag with Oscillatory Transients	C_{11}	200	99	99	99	98.3	99.8	99.25	99.3	98.9
Oscillatory Transients with Swell, and Sag	C_{12}	200	99	98	99	98.7	99.7	99.3	99.3	99
Classification Accuracy (%)			99	98.3	98.8	97.9	99.8	99.12	99.7	98.9

effective because small eigenvalues usually contain noise. After several simulation attempts, we came to the conclusion that the best value $\alpha = 3$ is chosen for the decomposition of PQDs. MSSA decomposition also extracts the most effective features and this technique performs adequately well to eradicate the noise.

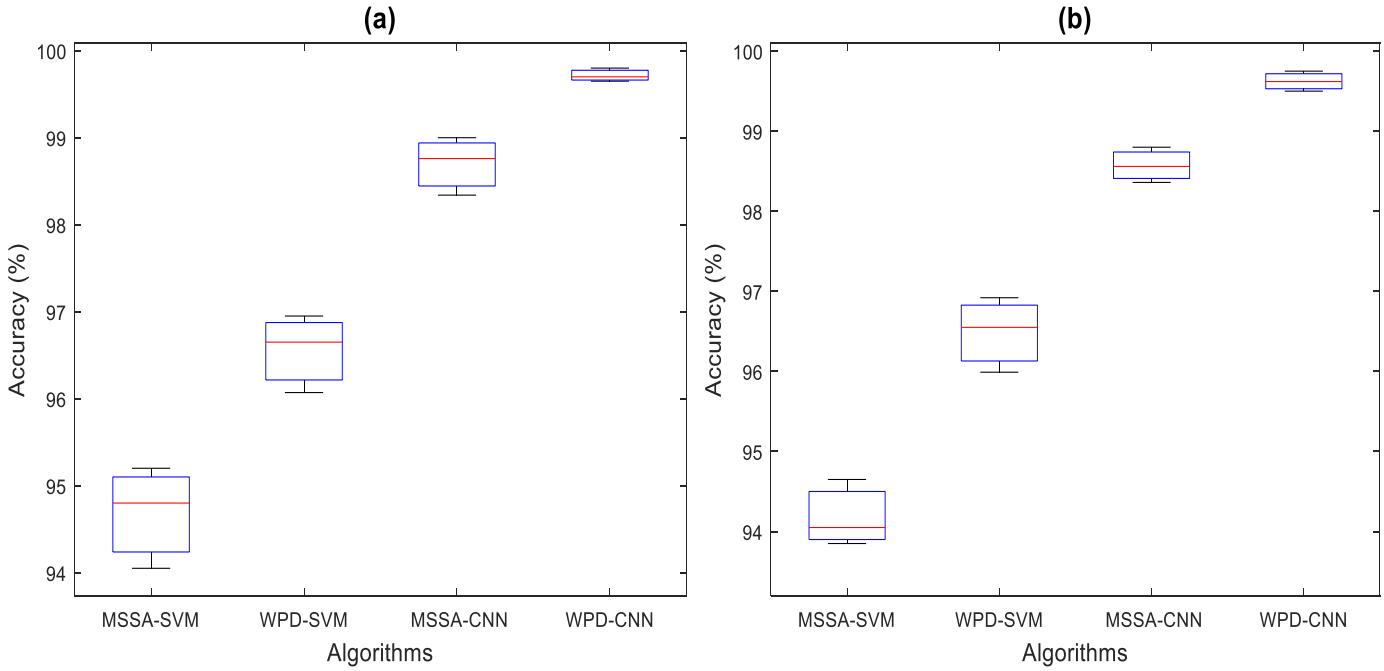

Figure 11. Accuracy comparison of proposed method with SVM classifier (a) dataset 1 (b) dataset 2

4.1. Accuracy comparison with SVM Classifier

The proposed feature extraction techniques have also been tested with support vector machine (SVM) classifier. The classification accuracies of MSSA, WPD with CNN based softmax and SVM classifiers respectively, are shown in Fig.11. It is observed that the MSSA and WPD with SVM has least classification accuracy as compared to MSSA and WPD with CNN classifier. The results of the proposed

algorithm validate that the proposed algorithm can be applied to the real system.

4.2 Computational Complexity

In this subsection, one of the important features of this study computational complexity is discussed. Figure 12 shows the computational complexity analysis of different datasets with SVM and CNN classifiers based algorithms. However, it can be observed from the figure that CNN based classifier algorithm has the least computational burden as compared to SVM classifier. On the other side, WPD has higher complexity due to in-detail analysis of frequency sub-bands. MSSA has less complexity due to the optimal value of α and less number of features are considered as compared to WPD. We can conclude that the MSSA is best-suited decomposition technique if we are considering the important factor of computational speed.

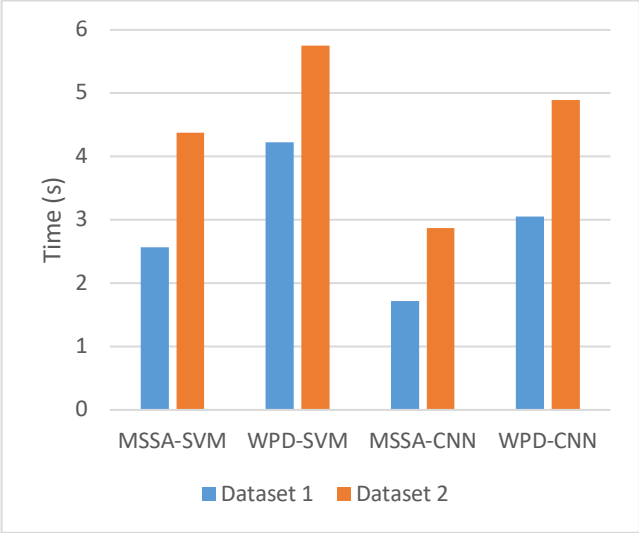

Figure 12. Comparison of Computational time (S) Complexity

Table 4. Performance comparison with recent articles.

Ref#	Classifier	Feature Extraction	No. of PQDs	Data type	Phase Type	Classification Accuracy (%)
[40]	SR-ELM	FTT	12	Real	3-∅	99.71
[41]	SVM	DWT, HST	9	Simulated and Real	3-∅	99.44
[42]	RF	MODWT, SGWT, ST	10	Simulated and Real	Single-∅	97.39
[43]	DTB	MSMGF, STMHT	10	Simulated and Real	Single-∅	99.7
Proposed	1-DCNN	MSSA, WPD	12	Synthetic, Simulated	3-∅	99.8

4.3. Performance Comparison

Table 4 presents a detailed comparison between published articles with the proposed algorithm. In [40], 12 types of single and multiple PQDs were considered and Fast time-time transform (FTT) with small residual extreme learning machine (SR-ELM) were successfully implemented but this method has relatively less classification accuracy than the proposed method. Only nine types of three-phase PQDs were classified with Discrete WT, hyperbolic ST, and SVM. The classification accuracy 99.44 was achieved [41]. However, this article considered less number of PQDs and having less classification accuracy as compared proposed algorithm.

In [42], maximum overlapping DWT (MODWT), second-generation WT (SGWT) and ST were compared to accomplish the best classification results. ST retained the best classification rate of 97.39%. only ten single-phase PQDs and multi-scale morphological gradient filter (MSMGF) and short-time modified Hilbert transform (STMHT) with decision tree-based (DTB) classifier were studied to achieve better classification results [43]. This comparative study shows that the proposed study attained higher classification results.

5. Conclusions

In this study, two feature extraction techniques (MSSA, WPD) have successfully examined with CNN based softmax and SVM classifiers in terms of classification accuracy and computational complexity. Two types of datasets for 12 type of single and multiple PQ disturbances were considered. The synthetic dataset has been generated from MATLAB R2017b and simulated dataset of three-phase PQ disturbance were generated from a modified IEEE 13 bus system with interconnection of wind distributive system. Three-phase PQDs were separated into single phase to analyze and extract the features. Six statistical parameters such as energy, entropy, standard deviation, mean, skewness, and kurtosis were considered to select the optimal features. The classification results show that WPD and CNN based softmax classifier has better accuracy among other comparative techniques. In CNN, dropout and ReLU were utilized to tune the data, which helps to improve the classification accuracy.

However, MSSA and CNN based softmax classifier method have less computational complexity. The SVM classifier and different range of Gaussian noises were also applied to validate the proposed algorithm. The higher classification accuracy validates that this study can also be applied to different applications such as images, facial detection, fault detection, and classification.

6. Funding

This work was supported by Jiangsu International Science and Technology Cooperation Project [BZ2017067], Jiangsu Provincial Key Research and Development Program [BE2018372], Jiangsu Natural Science Foundation [BK20181443], Zhenjiang City Key Research and Development Program [NY2018001], Qing Lan project of Jiangsu Province and the Priority Academic Program Development (PAPD) of the Jiangsu Higher Education Institutions, China

7. References

[1] J. N. Jiang, C. Y. Tang, and R. G. Ramakumar, "Control and Operation of Grid-Connected Wind Farms," *Advances in Industrial Control,* 2016.

[2] L. Mundaca, L. Neij, A. Markandya, P. Hennicke, and J. Yan, "Towards a Green Energy Economy? Assessing policy choices, strategies and transitional pathways," ed: Elsevier, 2016.

[3] T. Ackermann, *Wind power in power systems* vol. 140: Wiley Online Library, 2005.

[4] G. A. Rampinelli, F. P. Gasparin, A. J. Bühler, A. Krenzinger, and F. C. Romero, "Assessment and mathematical modeling of energy quality parameters of grid connected photovoltaic inverters," *Renewable and Sustainable Energy Reviews,* vol. 52, pp. 133-141, 2015.

[5] S. Mishra, C. Bhende, and B. Panigrahi, "Detection and classification of power quality disturbances using S-transform and probabilistic neural network," *IEEE Transactions on power delivery,* vol. 23, pp. 280-287, 2007.

[6] O. P. Mahela, A. G. Shaik, and N. Gupta, "A critical review of detection and classification of power quality events," *Renewable and Sustainable Energy Reviews,* vol. 41, pp. 495-505, 2015.

[7] C.-Y. Lee and Y.-X. Shen, "Optimal feature selection for power-quality disturbances classification," *IEEE Transactions on power delivery,* vol. 26, pp. 2342-2351, 2011.

[8] Y. Shen, M. Abubakar, H. Liu, and F. Hussain, "Power Quality Disturbance Monitoring and Classification Based on Improved PCA and Convolution Neural Network for Wind-Grid Distribution Systems," *Energies,* vol. 12, p. 1280, 2019.

[9] S. Santoso, W. M. Grady, E. J. Powers, J. Lamoree, and S. C. Bhatt, "Characterization of distribution power quality events with Fourier and wavelet transforms," *IEEE Transactions on Power Delivery,* vol. 15, pp. 247-254, 2000.

[10] G. Heydt, P. Fjeld, C. Liu, D. Pierce, L. Tu, and G. Hensley, "Applications of the windowed FFT to electric power quality assessment," *IEEE Transactions on Power Delivery,* vol. 14, pp. 1411-1416, 1999.

[11] P. S. Wright, "Short-time Fourier transforms and Wigner-Ville distributions applied to the calibration of power frequency harmonic analyzers," *IEEE transactions on instrumentation and measurement,* vol. 48, pp. 475-478, 1999.

[12] A. Gaouda, M. Salama, M. Sultan, and A. Chikhani, "Power quality detection and classification using wavelet-multiresolution signal decomposition," *IEEE Transactions on power delivery,* vol. 14, pp. 1469-1476, 1999.

[13] M. Uyar, S. Yildirim, and M. T. Gencoglu, "An effective wavelet-based feature extraction method for classification of power quality disturbance signals," *Electric Power Systems Research,* vol. 78, pp. 1747-1755, 2008.

[14] W. Tong, X. Song, J. Lin, and Z. Zhao, "Detection and classification of power quality disturbances based on wavelet packet decomposition and support vector machines," in *2006 8th International Conference on signal processing*, 2006.

[15] R. Vautard, P. Yiou, and M. Ghil, "Singular-spectrum analysis: A toolkit for short, noisy chaotic signals," *Physica D: Nonlinear Phenomena,* vol. 58, pp. 95-126, 1992.

[16] M. T. Chu, M. M. Lin, and L. Wang, "A study of singular spectrum analysis with global optimization techniques," *Journal of Global Optimization,* vol. 60, pp. 551-574, 2014.

[17] J. B. Elsner and A. A. Tsonis, *Singular spectrum analysis: a new tool in time series analysis*: Springer Science & Business Media, 2013.

[18] B. Muruganatham, M. Sanjith, B. Krishnakumar, and S. S. Murty, "Roller element bearing fault diagnosis using singular spectrum analysis," *Mechanical systems and signal processing,* vol. 35, pp. 150-166, 2013.

[19] D. H. Schoellhamer, "Singular spectrum analysis for time series with missing data," *Geophysical Research Letters,* vol. 28, pp. 3187-3190, 2001.

[20] J. Zabalza, J. Ren, Z. Wang, S. Marshall, and J. Wang, "Singular spectrum analysis for effective feature extraction in hyperspectral imaging," *IEEE Geoscience and Remote Sensing Letters,* vol. 11, pp. 1886-1890, 2014.

[21] S. Sanei, M. Ghodsi, and H. Hassani, "An adaptive singular spectrum analysis approach to murmur detection from heart sounds," *Medical engineering & physics,* vol. 33, pp. 362-367, 2011.

[22] H. Hassani and A. Zhigljavsky, "Singular spectrum analysis: methodology and application to economics data," *Journal of Systems Science and Complexity,* vol. 22, pp. 372-394, 2009.

[23] D. Salgado and F. Alonso, "Tool wear detection in turning operations using singular spectrum analysis," *Journal of Materials Processing Technology,* vol. 171, pp. 451-458, 2006.

[24] T. Chakravorti, R. Patnaik, and P. Dash, "A morphological filter based disturbance detection and classification technique for DFIG wind farm based microgrid," in *2015 IEEE Power, Communication and Information Technology Conference (PCITC)*, 2015, pp. 979-985.

[25] S. S. Kaddah, K. M. Abo-Al-Ez, T. F. Megahed, and M. G. Osman, "Probabilistic power quality indices for electric grids with increased penetration level of wind power generation," *International journal of electrical power & energy systems,* vol. 77, pp. 50-58, 2016.

[26] P. K. Ray, S. R. Mohanty, N. Kishor, and J. P. Catalão, "Optimal feature and decision tree-based classification of power quality disturbances in distributed generation systems," *IEEE Transactions on Sustainable Energy,* vol. 5, pp. 200-208, 2013.

[27] R. Deshpande, "Analysis of power quality variations in electrical distribution system with renewable energy sources," *International Journal of Renewable Energy Research (IJRER),* vol. 9, pp. 281-289, 2019.

[28] G. N. Baltas, C. Perales-González, P. Mazidi, F. Fernandez, and P. Rodríguez, "A Novel Ensemble Approach for Solving the Transient Stability Classification Problem," in *2018 7th International Conference on Renewable Energy Research and Applications (ICRERA)*, 2018, pp. 1282-1286.

[29] J. M. Malof, L. M. Collins, K. Bradbury, and R. G. Newell, "A deep convolutional neural network and a random forest classifier for solar photovoltaic array detection in aerial imagery," in *2016 IEEE International Conference on Renewable Energy Research and Applications (ICRERA)*, 2016, pp. 650-654.

[30] M. H. Dhend and R. H. Chile, "Fault diagnosis methodology in smart grid with distributed energy generation," in *2016 IEEE International Conference on Renewable Energy Research and Applications (ICRERA)*, 2016, pp. 885-890.

[31] W. H. Kersting, "Radial distribution test feeders," *IEEE Transactions on Power Systems,* vol. 6, pp. 975-985, 1991.

[32] H. Liu, F. Hussain, Y. Shen, S. Arif, A. Nazir, and M. Abubakar, "Complex power quality disturbances classification via curvelet transform and deep learning," *Electric Power Systems Research,* vol. 163, pp. 1-9, 2018.

[33] C. E. Heil and D. F. Walnut, "Continuous and discrete wavelet transforms," *SIAM review,* vol. 31, pp. 628-666, 1989.

[34] J. Wang and C. Wang, "A classification method of power quality disturbance based on wavelet packet decomposition," in *2004 IEEE Region 10 Conference TENCON 2004.*, 2004, pp. 244-247.

[35] W. Hu, Y. Huang, L. Wei, F. Zhang, and H. Li, "Deep convolutional neural networks for hyperspectral image classification," *Journal of Sensors,* vol. 2015, 2015.

[36] S. Kiranyaz, T. Ince, and M. Gabbouj, "Real-time patient-specific ECG classification by 1-D convolutional neural networks," *IEEE Transactions on Biomedical Engineering,* vol. 63, pp. 664-675, 2015.

[37] C. Szegedy, W. Liu, Y. Jia, P. Sermanet, S. Reed, D. Anguelov*, et al.*, "Going deeper with convolutions," in *Proceedings of the IEEE conference on computer vision and pattern recognition*, 2015, pp. 1-9.

[38] N. Srivastava, G. Hinton, A. Krizhevsky, I. Sutskever, and R. Salakhutdinov, "Dropout: a simple way to prevent neural networks from overfitting," *The journal of machine learning research,* vol. 15, pp. 1929-1958, 2014.

[39] M. K. Saini and R. Kapoor, "Classification of power quality events–a review," *International Journal of Electrical Power & Energy Systems,* vol. 43, pp. 11-19, 2012.

[40] M. K. Saini and R. K. Beniwal, "Detection and classification of power quality disturbances in wind-grid integrated system using fast time-time transform and small residual-extreme learning machine," *International Transactions on Electrical Energy Systems,* vol. 28, p. e2519, 2018.

[41] M. Hajian and A. A. Foroud, "A new hybrid pattern recognition scheme for automatic discrimination of power quality disturbances," *Measurement,* vol. 51, pp. 265-280, 2014.

[42] S. Upadhyaya, S. Mohanty, and C. Bhende, "Hybrid methods for fast detection and characterization of power quality disturbances," *Journal of Control, Automation and Electrical Systems,* vol. 26, pp. 556-566, 2015.

[43] T. Chakravorti, R. K. Patnaik, and P. K. Dash, "Detection and classification of islanding and power quality disturbances in microgrid using hybrid signal processing and data mining techniques," *IET Signal Processing,* vol. 12, pp. 82-94, 2017.